TASK QUARTERLY 13 No 3, 199–206

FEATURES OF LIGHT SCATTERING BY SURFACE FRACTAL STRUCTURES

O. YU. SEMCHUK, L. G. GRECHKO, D. L. VODOPIANOV AND L. YU. KUNITSKA

Institute of Surface Chemistry,
National Academy of Sciences of Ukraine,
Gen. Naumov str. 17, 03164, Kyiv, Ukraine
inchem@mail.kar.net

(Received 2 March 2009; revised manuscript received 16 June 2009)

Abstract: The average coefficient of light scattering by surface fractal structures is calculated within the limits of the Kirchhoff method. A normalized band-limited Weierstrass function is presented for modeling 2D fractal rough surfaces. On the basis of the numerical calculation of the average scattering coefficient, scattering indicatrices diagrams are calculated for various surfaces and falling angles. An analysis of the diagrams leads to the following conclusions: the scattering is symmetric relatively to the plane of fall; the picture becomes complicated when the surface calibration degree is increased; the greatest intensity of a scattering wave is observed in the mirroring direction; there are other directions in which bursts of intensity are observed.

Keywords: fractal, scattering, light, electromagnetic wave, scattering coefficient, rough surface

Notation

$h = z(x,y)$ – ensemble averaging over surfaces [m];
$I_l(z)$ – Bessel function of integer order;
k – wave vector of incident wave [m^{-1}];
$\vec{E}_s$ – electric field of scattering wave [Vm^{-1}].

Greek symbols

θ_1 – incident angles [degrees];
θ_2 – polar angle [degrees];
θ_3 – horizontal angle [degrees];
σ – profile height [m];
λ – wave-length [m].

Subscripts

s – scattering index;
e – external;
f – describes the edge effects.

1. Introduction

Accurate measurement of surface roughness of machined work pieces is of fundamental importance particularly in the precision engineering and manufacturing industry. This is mainly due to more stringent demands on the material quality and because of miniaturization of product components in these industries [1–3]. In the disk drive industry, for instance, the disk surface roughness should be accurately measured and controlled to maintain the quality of the electrical components mounted on an optical disk. Hence, the surface finish, normally expressed in terms of surface roughness, is a critical parameter used for acceptance or rejection of a product.

Surface roughness is usually determined by a mechanical stylus profilometer. However, the stylus technique has certain limitations: the mechanical contact between the stylus and the object can cause deformations or damage on the specimen surface. Hence, it is a pointwise and time consuming measurement method. Therefore, a noncontact faster optical method would be attractive. Different optical noncontact methods are developed for measuring surface roughness. They are based mainly on reflected light detection, focus error detection, laser scattering, speckle, and interference [4–10]. Some of these methods have a good resolution and are applied in some sectors where mechanical measuring methods previously enjoyed clear predominance. Among these methods, the light scattering method [11] which is a noncontact area-averaging technique is potentially faster for surface inspection than other techniques, particularly the traditional stylus technique. Other commercially available products such as the Atomic Force Microscope (AFM) and subwavelength photoresist gratings [12–15] are pointwise techniques used mainly for optically smooth surfaces with roughness in a nanometer range.

In this paper the average coefficient of light scattering by surface fractal structures is calculated within the limits of the Kirchhoff method. A normalized band-limited Weierstrass function is used for modeling 2D fractal rough surfaces. On the base of numerical calculating of the average scattering coefficient, the scattering indicatrices diagrams for various surfaces and incidence angles are obtained. An analysis of the diagrams results in the following conclusions: the scattering is symmetrical relatively to the plane of fall; the picture becomes complicated when the surface calibration degree is increased; the greatest intensity of a scattering wave is observed in the mirroring direction; there are other directions in which bursts of intensity are observed.

2. Fractal-like model for two-dimensional rough surfaces

The modified two-dimensional Weierstrass function is taken in the form:

$$z(x,y) = c_w \sum_{n=0}^{N-1} \sum_{m=1}^{M} q^{(D-3)n} \sin\left\{ K q^n \left[x\cos\frac{2\pi m}{M} + y\sin\frac{2\pi m}{M} \right] + \varphi_{nm} \right\}, \qquad (1)$$

where c_w is a constant which ensures that $z(x,y)$ has a unit perturbation amplitude; q ($q>1$) is the fundamental spatial frequency; D ($2<D<3$) is the fractal dimension; K is the fundamental wave number; N and M are the number of overtones, and φ_{nm} are phase terms that have a uniform distribution over the interval $[-\pi,\pi]$.

The above function is a combination of determinate periodic and random constituents. The function is anisotropic in both directions, given M and N are not too large. It is self-similar and it has a large derivative. The function presents a multi-scale surface with the same roughness down to some fine scales. Since natural surfaces are generally neither purely random nor purely periodic, and often anisotropic, the function proposed is a good candidate for modeling natural surfaces.

The phases φ_{nm} can be chosen in appointed or casual ways, what gives deterministic or stochastic $z(x,y)$ function, respectively. Later on, the functions ϕ_{nm} are considered as casual values distributed regularly on the segment $[-\pi;\pi]$. Particular realization of function $z(x,y)$ (with the meanings of parameters c_w, q, K, D, N, M chosen beforehand) can be received with each particular choice of numerical values of all $N \times M$ phases ϕ_{nm} (for example, with the help of a random-number generator). Every possible realization of function $z(x,y)$ forms an ensemble of surfaces.

Deflection of the rough surface points from a basic plane appears to be proportional to the c_w value, therefore, this parameter is connected with the height of structure imperfections over the surface. Later on, it is found more convenient to set a rough surface by choosing the root-mean-square height of its profile σ which can be calculated using the expression:

$$\sigma \equiv \sqrt{\langle h^2 \rangle}, \tag{2}$$

where $h = z(x,y)$, $\langle \ldots \rangle = \prod_{n=0}^{N-1} \prod_{m=1}^{M} \int_{-\pi}^{\pi} \frac{d\varphi_{nm}}{2\pi} (\ldots)$ means ensemble averaging over the surfaces.

The connection between c_w and σ can be established taking the integrals directly:

$$\sigma = \left[\prod_{n=0}^{N-1} \prod_{m=1}^{M} \int_{-\pi}^{\pi} \frac{d\varphi_{nm}}{2\pi} z^2(x,y) \right]^{\frac{1}{2}} = c_w \left[\frac{M\left(1-q^{2N(D-3)}\right)}{2\left(1-q^{2(D-3)}\right)} \right]^{\frac{1}{2}}. \tag{3}$$

Thus, the rough surface in the accepted model is described by the function with six parameters: c_w (or σ), q, K, D, N, M. The influence of different parameters on the appearance of a surface can be investigated analytically by studying the profiles of surfaces on the base of the results of Weierstrass function numerical calculations. Thus, it is found out that:

- the wave number K determines the wave length of the surface's fundamental harmonic;
- the numbers N, M, D and q determine the surface calibration degree because of imposing additional harmonics on the fundamental wave, and N and M determine the number of harmonics imposed;
- D determines the amplitude of harmonics;
- q determines both the amplitude and frequency of harmonics.

It should be noticed that the large scale spatial heterogeneity of the surface increases, too with an increase in N, M, D and q.

3. Light scattering on surface fractal structures

A scheme of the experiment on light scattering is presented in Figure 1. The initial wave falls on a rough surface S at the prescribed angle and scatters in all directions. The scattering wave is observed by means of detector D in the direction which is characterized by polar angle θ_2 and horizontal angle θ_3. The measured magnitude is the intensity of light I_3 scattered in the direction (θ_2,θ_3). The purpose is to obtain a scattering indicatrix of the electromagnetic wave (light) after its interaction with a fractal surface (1).

While $I_s = \vec{E}_s \cdot \vec{E}_s^*$ (where $\vec{E}_s$ is an electric field of the scattering wave in complex representation) the problem of finding I_s is reduced to finding a scattered field $\vec{E}_s$. This field is to be found using the Kirchhoff method [16]. Considering the complexity of the problem, the advantage of a simpler scalar variant of the theory is preferred, according to which the electromagnetic field is described by a scalar value. Thus, an opportunity is lost to analyze the polarizing effects.

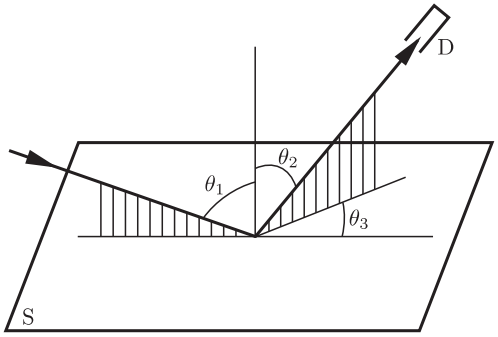

Figure 1. Scheme of experiment on light scattering by fractal surface: S is a scattering surface; D – detector, θ_1 is a light angle; θ_2 is a polar angle; θ_3 is a horizontal angle.

Using the base formula of the Kirchhoff method it is possible to find the scattered field under the following conditions:

- the incident wave is monochromatic and plane;
- the scattered surface is rough inside a rectangle $(-X < x_0 < X,\ -Y < y_0 < Y)$ and smooth outside the borders;
- the size of the rough site is much larger than the length of the incident wave;
- all points of the surface have a complete gradient;
- the reflection coefficient is the same at all points of the surface;
- the scattering field is observed in the wave zone, *i.e.*, far enough from the scattering surface.

Under these conditions, the scattered field can be expressed by the following formula:

$$E_s(\vec{r}) = -ikrF(\theta_1,\theta_2,\theta_3)\frac{e^{ikr}}{2\pi r}\int\limits_{S_0} \exp\left[ik\varphi(x_0,y_0)\right]dx_0dy_0 + E_e(\vec{r}), \tag{4}$$

where k is a wave number of the incident wave; $F(\theta_1,\theta_2,\theta_3) = -\frac{R}{2C}(A^2+B^2+C^2)$ is an angle factor; R is a scattering coefficient; $\varphi(x_0,y_0) = Ax_0 + By_0 + Ch(x_0,y_0)$

is a phase function; $h(x_0,y_0)=z(x_0,y_0)$; $A=\sin\theta_1-\sin\theta_2\cos\theta_3$; $B=-\sin\theta_2\sin\theta_3$; $C=-\cos\theta_1-\cos\theta_2$;

$$E_e(\vec{r})=-\frac{R}{C}\cdot\frac{e^{ikr}}{4\pi r}(AI_1+BI_2);$$

$$\begin{aligned} I_1&=\int\limits_{-Y}^{Y}\left[e^{ik\phi(X,y_0)}-e^{ik\phi(-X,y_0)}\right]dy_0,\\ I_2&=\int\limits_{-X}^{X}\left[e^{ik\phi(x_0,Y)}-e^{ik\phi(x_0,-Y)}\right]dx_0. \end{aligned} \tag{5}$$

Having taken integrals (4) and (5) using the formula:

$$e^{iz\sin\phi}=\sum_{l=-\infty}^{\infty}I_l(z)e^{il\phi},$$

where $I_l(z)$ is the Bessel function of integer order, it is possible to obtain:

$$\begin{aligned} E_s(\vec{r})=-2ikFXY\frac{e^{ikr}}{\pi r}\sum_{l_{\{rs\}}}\left\{\left[\prod_{uv}I_{l_uv}(\xi_u)\right]\exp\left[i\sum_{nm}l_{nm}\varphi_{nm}\right]\right\}\times\\ \times\operatorname{sinc}(k_cX)\operatorname{sinc}(k_sY)+E_e(\vec{r}) \end{aligned} \tag{6}$$

where

$$F=F(\theta_1,\theta_2,\theta_3),$$

$$\sum_{l_{\{rs\}}}\equiv\sum_{l_{0,1}=-\infty}^{\infty}\sum_{l_{0,2}=-\infty}^{\infty}\cdots\sum_{l_{(N-1),M}=-\infty}^{\infty},\qquad\prod_{uv}\equiv\prod_{u=1}^{N-1}\prod_{v=0}^{M},\qquad\sum_{nm}\equiv\sum_{n=1}^{N-1}\sum_{m=0}^{M},$$

$$\xi_u\equiv kc_wCq^{(D-3)u},\qquad\operatorname{sinc}x\equiv\frac{\sin x}{x},$$

$$k_c\equiv kA+K\sum_{nm}q^nl_{nm}\cos\frac{2\pi m}{M},\qquad k_s\equiv kB+K\sum_{nm}q^nl_{nm}\sin\frac{2\pi m}{M},$$

$$E_e(\vec{r})=-ikXY\frac{R}{C}\left(A^2+B^2\right)\frac{e^{ikr}}{\pi r}\operatorname{sinc}(kAX)\operatorname{sinc}(kBY).$$

Thus, the expression (6) makes it possible to solve, within the limits of the Kirchhoff method, the problem of finding field scattering by a fractal surface.

Now, using formula (4) it is possible to calculate the scattered wave intensity after setting the parameters of the dispersive surface c_w (or) σ, D, q, K, N, M, X, Y, ϕ_{nm}, parameter k (or $\lambda=\frac{2\pi}{k}$) of the incident wave, also parameters θ_1, θ_2, θ_3 describing the experiment geometry. This intensity characterizes scattering on particular realization of surface $z(x,y)$ (with a particular set of casual phases ϕ_{nm}). To compare the calculations with the experimental data it is necessary to operate with the average intensity on the ensemble of surfaces $\langle I_s\rangle=\left\langle\vec{E}_s\vec{E}_s^{\,*}\right\rangle$. Such intensity appears to be proportional to the intensity $I_0=\left(\frac{2kXY\cos\theta_1}{\pi r}\right)^2$ of the wave reflected

from the corresponding smooth basic surface, therefore, it is more convenient for a theoretical analysis of the results to use the average scattering coefficient:

$$\langle \rho_s \rangle = \frac{\langle I_s \rangle}{I_0}.$$

Having calculated $\langle I_s \rangle$ and using Equation (6), an exact expression can be obtained:

$$\begin{aligned}\langle \rho_s \rangle = &\left[\frac{F(\theta_1,\theta_2,\theta_3)}{\cos\theta_1}\right]^2 \sum_{l_{\{rs\}}} \left\{ \prod_{uv} I^2_{l_{uv}}(\xi_u) \operatorname{sinc}^2(k_c X) \operatorname{sinc}^2(k_s Y) \right\} + \\ &+ \left[\frac{R(A^2+B^2)}{2C\cos\theta_1}\right]^2 \operatorname{sinc}^2(kAX) sinc^2(kBY).\end{aligned} \tag{7}$$

While the expression (7) contains an infinite sum, using it for numerical calculations appears to be inconvenient. An essential simplification can be reached in case $\xi_n < 1$. Using the Bessel function expansion in the series:

$$I_\nu(z) = \left(\frac{3}{2}\right)^\nu \sum_{k=0}^{\infty} \frac{(-z^2/4)^k}{k!\Gamma(\nu+k+1)}, \tag{8}$$

and neglecting members of orders greater than ξ_n^2, an approximate expression can be obtained for the average scattering coefficient:

$$\begin{aligned}\langle \rho_s \rangle \approx &\left[\frac{F(\theta_1,\theta_2,\theta_3)}{\cos\theta_1}\right]^2 \left\{ \left[1-(k\sigma C)^2\right] \operatorname{sinc}^2(kAX) \operatorname{sinc}^2(kBY) + \right. \\ &\left. + \frac{1}{2} c_f^2 \sum_{nm} q^{2(D-3)n} \operatorname{sinc}^2\left[\left(kA + Kq^n \cos\frac{2\pi m}{M}\right)X\right] \sin^2\left[\left(kB + Kq^n \sin\frac{2\pi m}{M}\right)Y\right] \right\} + \\ &+ \left[\frac{R}{2C\cos\theta_1}\left(A^2+B^2\right)\right]^2 \operatorname{sinc}^2(kAX) \operatorname{sinc}^2(kBY),\end{aligned} \tag{9}$$

where

$$c_f \equiv k c_w C = k\sigma C \left[\frac{2}{M} \cdot \frac{1-q^{2(D-3)}}{1-q^{2N(D-3)}}\right]^{\frac{1}{2}}.$$

4. Numerical results

On the base of expressions (1) and (9), using the original program developed within the *Mathematica 5.1* complex, a numerical surface modeling is realized on the base of the Weierstrass function, an average scattering coefficient is calculated, and diagrams of normalizable scattering indicatrices versus polar (θ_2) and horizontal (θ_3) scattering angles for different fractal surfaces and incident angles θ_1 are created. A root-mean-square value σ, a surface's fundamental wave number K, and dimensions X, Y of the surface fragment are expressed with the aid of k-units because the wave number k of the incident wave is used in form of combinations $k\sigma$, kX, and kY. The Frenel reflection coefficient for a surface is taken as $R = 1$. Examples of typical scattering indicatrices are shown in Figure 2.

5. Conclusions

An analysis of the scattering coefficient $\ln\langle \rho_s \rangle$ versus scattering angles θ_2 and θ_3 diagrams for various fractal surface types and incident angles $\theta_1 = 30°$, $40°$, and $60°$ shown in Figure 2 leads to the following conclusions:

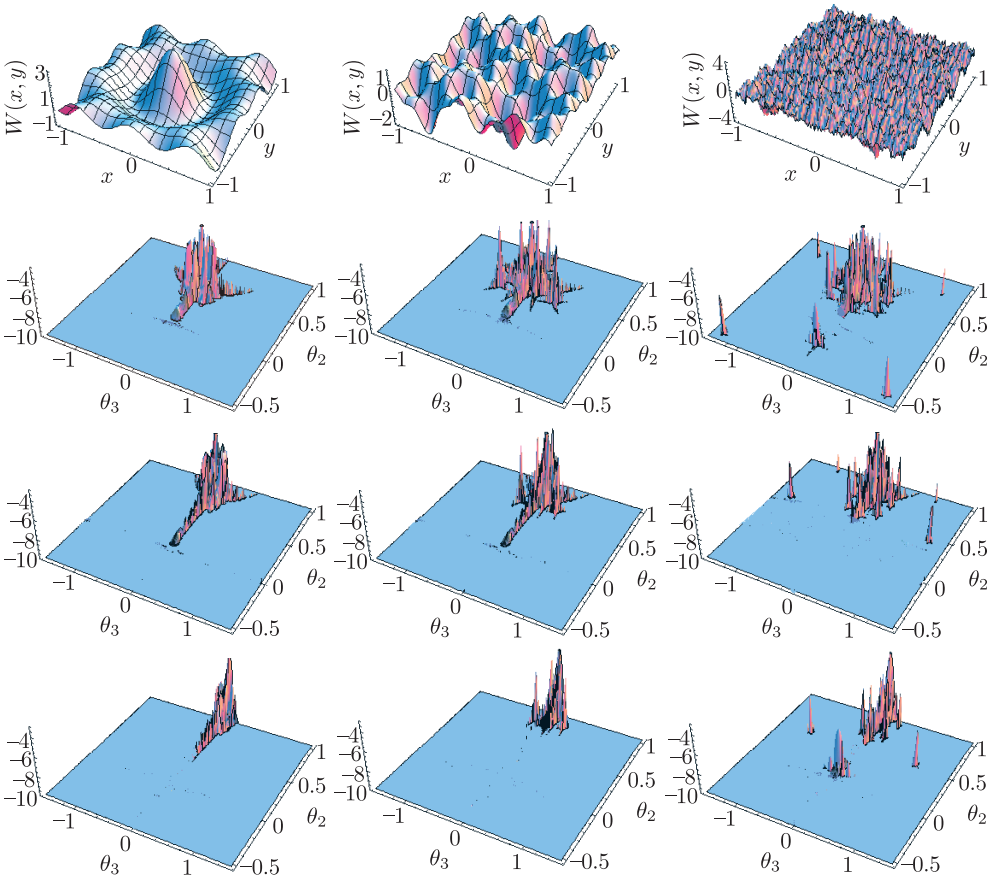

Figure 2. Scattering indicatrix $\log\langle\rho_s\rangle$ versus scattering angles θ_2 and θ_3 for various types of fractal surfaces. The first row of the diagram shows examples of rough surfaces for which scattering indicatrices are calculated. The variation of scattering indicatrix magnitude for three incident angles $\theta_1 = 30°$, $40°$, $60°$ (from left to right), and parameters: (1) $N = 5$, $M = 10$, $D = 2.9$, $q = 1.1$; (2) $N = 2$, $M = 3$, $D = 2.5$, $q = 3$; (3) $N = 5$, $M = 10$, $D = 2.5$, $q = 3$ is shown from top to bottom rows

1. The scattering is symmetrical concerning the plane of incidence.
2. The greatest intensity of the scattering wave is observed in a mirroring direction; there are other directions in which bursts of intensity are observed.
3. The picture becomes complicated when the surface calibration degree (or its spatial non-homogeneity) is increased: the number of peaks with the greatest intensity increases and additional peaks appear with smaller intensity and they are symmetric with respect to the plane of incidence.
4. Irrespective of the scattering surface type (fractal structure), another dependence of the scattering coefficient from the electromagnetic wave's incident angle is observed: the number of additional peaks diminishes with the incident angle increasing from 30° to 60°. The greatest number of them is observed at incident angle $\theta_1 = 30°$. It seems to be connected with influence of the height of the surface imperfections on the wave scattering process. When the incident

angle increases, the incident wave as though "stops to notice" the height of imperfections, so their contribution diminishes.

The registered scattering peculiarities are a consequence of a combination of both the chaotic character and self-similarity of a scattering rough fractal surface.

References

[1] Bifano T G, Fawcett H E and Bierden P A 1997 *Precis. Eng.* **20** (1) 53
[2] Wilkinson P, Kidd S R and Hand D P 1997 *Wear* **25** (1)
[3] Sherrington I and Smith E H 1986 *Precis. Eng.* **8** (2) 79
[4] Kaneami J and Hatazawa T 1989 *Wear* **134** 221
[5] Mitsui K 1986 *Precis. Eng.* **8** (40) 212
[6] Baumgart J W and Truckenbrodt H 1998 *Opt. Eng.* **37** (5) 1435
[7] Tay C J, Toh S L, Shang H M and Zhang J B 1995 *Appl. Opt.* **34** (13) 2324
[8] Peiponen K E and Tsuboi T 1990 *Opt. Laser Technol.* **22** (2) 127
[9] Whitley J Q, Kusy R, Mayhew P M J and Buckthat J E 1987 *Opt. Laser Technol.* **19** (4) 189
[10] Mitsui M, Sakai A and Kizuka O 1988 *Opt. Eng.* **27** (6) 498
[11] Vorburger T V, Marx E and Lettieri T R 1993 *Appl. Opt.* **32** (19) 3401
[12] Raymond C J, Murnane M R H, Naqvi S S and Mcneil J R 1995 *J. Vac. Sci. Technol. B* **13** (4) 1484
[13] Whitehouse D J 1991 *Meas. Control* **24** (3) 37
[14] Madsen L L, Srgensen J, Carneiro F K and Nielsen H S 1993–1994 *Metrologia* **30** 513
[15] Stedman M 1992, in *Proc. Int. Congr. X-ray Optics and Microanalysis*, IOP Publishing Ltd, Manchester 347
[16] Berry M V and Levis Z V 1980 *Proc. Royal Soc. London A* **370** 459